Applied Materials Today 1 (2015) 27–32

Contents lists available at ScienceDirect

Applied Materials Today

journal homepage: www.elsevier.com/locate/apmt

Short Communication

One-pot synthesis of graphene-molybdenum oxide hybrids and their application to supercapacitor electrodes

Rossella Giardi[a,b,c,*], Samuele Porro[b,c], Teya Topuria[a], Leslie Thompson[a], Candido Fabrizio Pirri[b,c], Ho-Cheol Kim[a]

[a] IBM Research Division, Almaden Research Center, 650 Harry Road, San Jose, CA 95120-6099, United States
[b] Politecnico di Torino, Applied Science and Technology Department, Corso Duca degli Abruzzi 24, 10129 Torino, Italy
[c] Istituto Italiano di Tecnologia, Center for Space Human Robotics@PoliTo, C.so Trento 21, 10129 Torino, Italy

ARTICLE INFO

Article history:
Received 19 June 2015
Received in revised form 10 August 2015
Accepted 10 August 2015

Keywords:
Supercapacitors
Sodium ions
Metal oxide
Graphene

ABSTRACT

Electrochemical double-layer capacitor (EDLC) electrodes are conventionally based on carbon materials, which provide increased chemical stability and the possibility of a large number of charge and discharge cycles. However, their specific capacitance is generally much lower than pseudo-capacitors based on metal oxide or conductive polymer electrodes. Carbon-based electrodes for electrochemical devices can be hybridized with metal oxide functionalities in order to provide catalytic activity that increases their electrochemical performances. We report the preparation of a conductive hybrid electrode of reduced graphene oxide and molybdenum oxide by a facile one-pot hydrothermal synthesis. A three-dimensional network structure comprising graphene and molybdenum oxide was obtained when phosphomolybdic acid was used as a precursor for molybdenum oxide. The hybrid material contains polycrystalline nanoparticles of molybdenum (IV) oxide (MoO_2) that covers the surface of reduced graphene oxide. Compared to graphene electrodes, the hybrid electrodes showed significantly improved specific capacitance, as good as three times higher (381 vs. 140 F/g), and considerable reduction of the equivalent series resistance (by about half) when they were used in a supercapacitor with sodium containing aqueous electrolyte.

1. Introduction

Energy storage holds the promise to provide a variety of benefits across the entire energy delivery value chain ranging from generation to delivery (transmission and distribution) to consumption [1,2]. While a number of different types of storage technologies exist today, electrochemical method has been dominating for consumer related applications [3]. Electrochemical energy storage, in general, relies on two types of devices, namely batteries and capacitors. Electrodes are a common component of the two devices, which connect the external electric circuit to the electrochemical cell. The correlation between materials, structures and performance of the electrodes, therefore, has been of great interest [4,5]. Carbons have been used as a common electrode material due to their abundance, wide electrochemical window, low cost, etc. Indeed a variety of carbons (glassy carbon, graphite, carbon black powder, carbon nanotube, graphene, etc.) have been studied as electrode materials [6,7]. Often the carbons are hybridized with functional materials to improve their electrochemical performance [8–10].

Here we report the synthesis and electrochemical characteristics of a carbon hybrid, which contains molybdenum oxide and reduced graphene oxide. We used a hydrothermal synthesis, which provides a reduced graphene oxide (RGO) and molybdenum oxide hybrid through a facile one-pot process. The structure of the hybrid material was carefully characterized using electron microscopy (SEM and TEM), X-ray diffraction (XRD), X-ray photoelectron spectroscopy (XPS) and Micro-Raman spectroscopy. The hybrid was applied to the electrode of a supercapacitor containing an aqueous electrolyte. The electrochemical performance of the hybrid electrodes in a Na^+ containing electrolyte is discussed in this report.

2. Materials and methods

Commercial reagents were used without further purification. Graphene Oxide (GO, thickness 0.7–1.2 nm) was purchased from ACS Materials (USA). Phosphomolybdic acid (PMA) solution of

* Corresponding author at: Politecnico di Torino, Applied Science and Technology Department, Corso Duca degli Abruzzi 24, 10129 Torino, Italy.
E-mail address: Rossella.Giardi@polito.it (R. Giardi).

http://dx.doi.org/10.1016/j.apmt.2015.08.001
2352-9407/

20 wt% in ethanol, poly(tetrafluoroethylene) (PTFE), and Na_2SO_4 were purchased from Sigma–Aldrich. The electrolyte was prepared by dissolving Na_2SO_4 in deionized (DI) water.

The GO powder was dispersed in DI water at room temperature using a Branson ultrasonic bath cleaner until the particulates were not visible. 0.5 g of PMA solution was added to the GO in DI water dispersion (2 mg/ml for 12 ml total volume) and ultrasonicated for 15 min. After sonication, the solution was transferred in a Teflon lined stainless steel autoclave with total volume of 18 ml and placed in a vacuum oven at a temperature of 180 °C for 16 h. After the hydrothermal reaction, when the autoclave reached room temperature, the samples were frozen using liquid nitrogen and dried overnight under vacuum.

The structure of the hybrid was characterized by using a FEI Helios Nanolab 400S field emission FIB/SEM and, an JEOL JEM-ARM200F STEM Cs-corrected cold FEG atomic resolution analytical microscope with GIF Quantum post-column energy filter and JEOL Centurio SDD EDS (silicon drift detector energy dispersive spectrometer). For X-ray photoelectron spectroscopy (XPS), a Physical Electronics Quantum ESCA Microprobe with a monochromated Al Kα X-ray source was used (200 mm spot size throughout and charge neutralization was used). 1000 eV survey spectra (187 eV pass energy, 1.6 eV/step) and high-resolution spectra (47 eV PE, 0.4 eV/step) were obtained from the XPS. The crystalline phase was analyzed with a Bruker D8 Discover X-ray diffractometer fitted with a 2-dimensional (2D) X-ray detector. All scans were performed

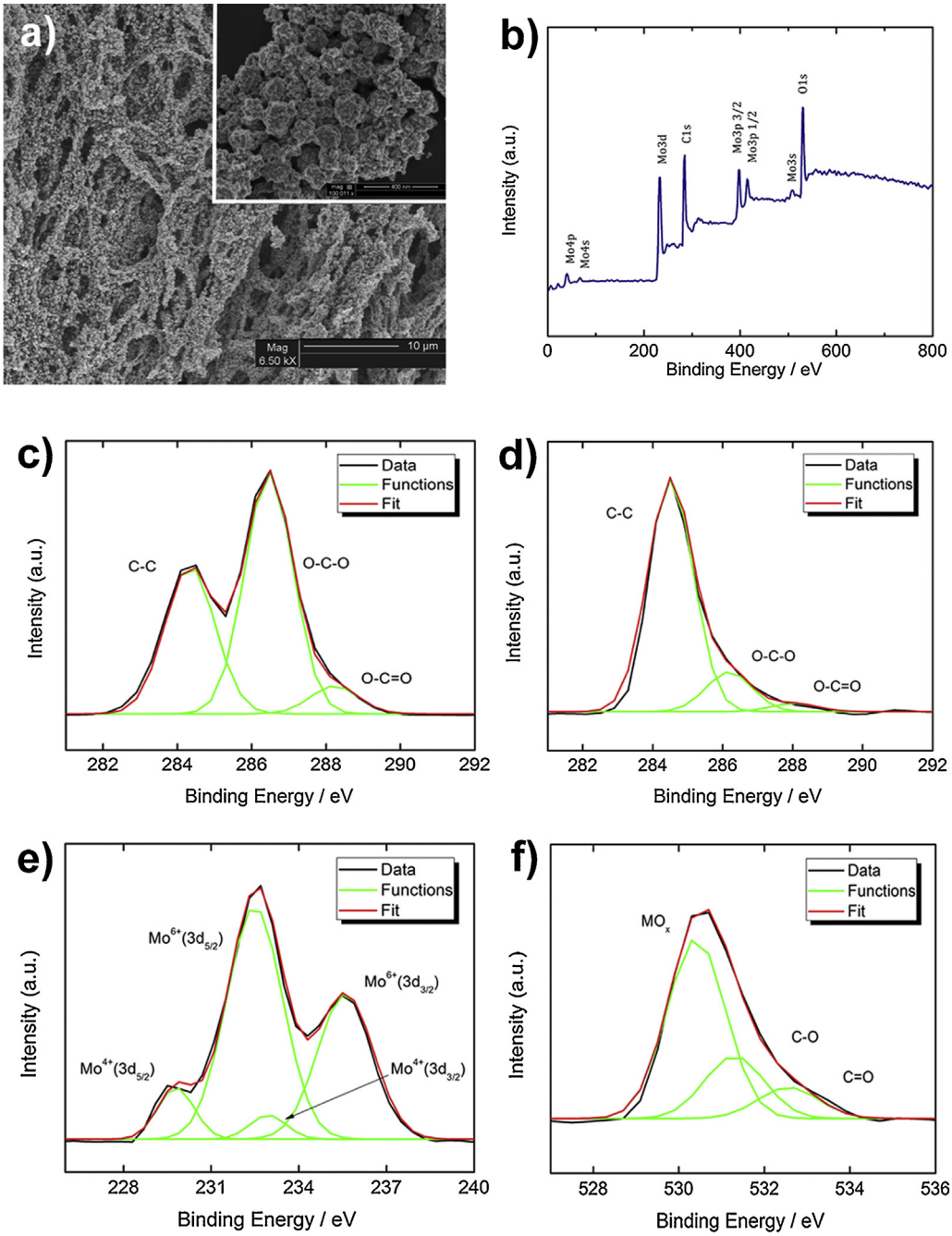

Fig. 1. (a) SEM micrograph of RGO/molybdenum oxide hybrid synthesized by the hydrothermal process. The inset shows high magnification image revealing particles of molybdenum oxide on graphene surface. (b) XPS survey spectrum of the hybrid. (c) Deconvolution of C1s high-resolution spectra of the pristine GO. Deconvolution of (d) C1s, (e) Mo3d and (f) O1s high-resolution spectra of the hybrid.

with the detector and incident beam in a symmetric θ–2θ geometry using graphite monochromated Cu-Kα X-rays (λ = 1.5418 Å), collimated on the sample in a pin-hole collimator to yield an X-ray beam diameter of ~650 μm. The structure of the hybrid was further analyzed by Micro-Raman spectroscopy, using a Thermo Scientific DXR with 532 nm incident photons in a range of 160–3400 cm^{-1} for the large scan and 160–1100 cm^{-1} for the high-resolution data. To determine the weight ratio of the composition of the hybrids, thermal gravimetric analysis (TGA) was performed under air using an Auto TGA 2950 HR by TA Instruments (heating rate of 5 °C per minute was used).

A BioLogic multi-potentiostats/galvanostats/EIS VPS-300 was used for electrochemical characterizations. A home-made, symmetrical two-electrode cell was used. Electrodes were prepared using slurry of the active material and 1% PTFE in DI water (binder). A stainless steel mesh (100 mesh size) disc 12 mm in diameter was used as current collector. When the current collector was completely covered with the slurry, approximately 3 mg of the active material was loaded. The electrodes were dried overnight in a vacuum oven at 40 °C. As the reference electrode, a commercially available carbon black powder (KetjenBlack, KB) with 60% PTFE in DI water was used. A Whatman GF/c glass filter was used as a separator (diameter of 16 mm, thickness of 265 μm). 1 M Na_2SO_4 solution in DI water was used as an electrolyte. Approximately 600 μl of the electrolyte was loaded for each supercapacitor cell.

Galvanostatic charge–discharge (GCD), cyclic voltammetry (CV) and electron impedance spectroscopy (EIS) were performed to characterize the electrochemical behavior. GCD was performed at 0.06 and 0.16 A/g with cut-off potential of ±1.5 V. Scan rates of 0.5, 2 and 5 mV/s were used for the CV ranging from −1.5 V to 1.5 V. EIS was performed in a frequency range between 122 kHz and 100 mHz.

3. Results and discussion

The synthesis of sponge-like 3D structure of graphene oxide (GO) using hydrothermal method has been previously reported [11–14]. Our synthesis scheme reproduces the formation of 3D structure. The morphology of the hybrid is shown in a SEM micrograph in Fig. 1 (a). The hydrothermal synthesis provides 3D graphene structure where the surface of graphene is covered with particles of molybdenum oxide. Fig. 1 also reports the XPS spectra of the hybrid. The survey spectrum in Fig. 1 (b) indicates the presence of Mo. Fig. 1 (c) reports the high-resolution C1s spectrum of the pristine GO, showing high surface oxidation of the sheets. The analysis of C1s spectrum of the hybrid material (Fig. 1 (d)) suggests the reduction of GO during the hydrothermal synthesis in the presence of PMA: the decrease in the intensities of peaks related to oxygen functionalities O—C—O at 286.3 eV and O—C=O at 288.3 eV compared to the C—C peak at 284.5 eV is evident [15–18]. The deconvolution peaks of the Mo 3d spectrum, reported in Fig. 1 (e), shows the characteristic doublet of the Mo(4+) composed by Mo $3d_{5/2}$ peak located at 229.8 eV and the Mo $3d_{3/2}$ peak at 232.9 eV, with a characteristic difference in binding energy of 3.1 eV [19–21]. This suggests that the Mo (IV) oxidation state of molybdenum oxide was synthesized by the hydrothermal method [22]. Nevertheless, the pronounced doublet at 232.4 eV and 235.6 eV is instead characteristic of Mo (VI) oxidation state and indicates mixed oxidation state of the molybdenum oxide, presumably resulting from surface

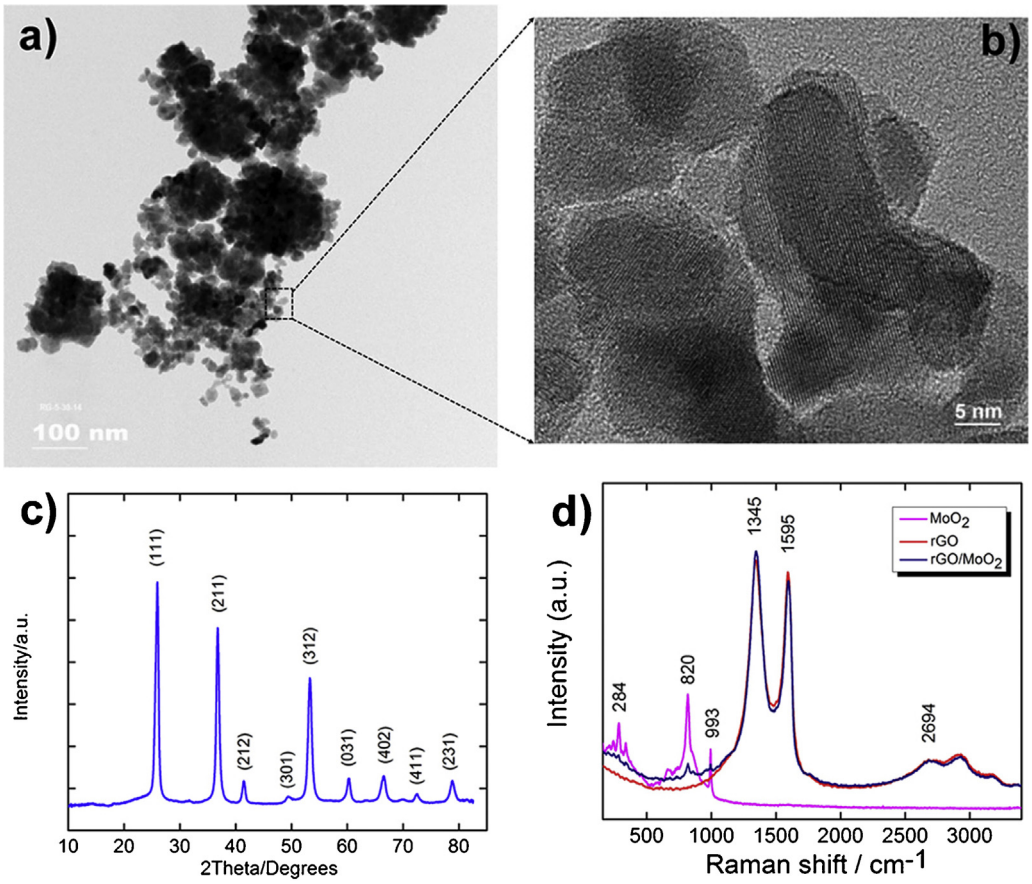

Fig. 2. (a) Low- and (b) high-resolution bright field TEM of the molybdenum oxide nanoparticles; (c) X-ray diffraction spectra of the molybdenum oxide. Samples were collected from the bottom on hydrothermal reactor. (d) Micro-Raman spectra of RGO, MoO_2 and the hybrid material.

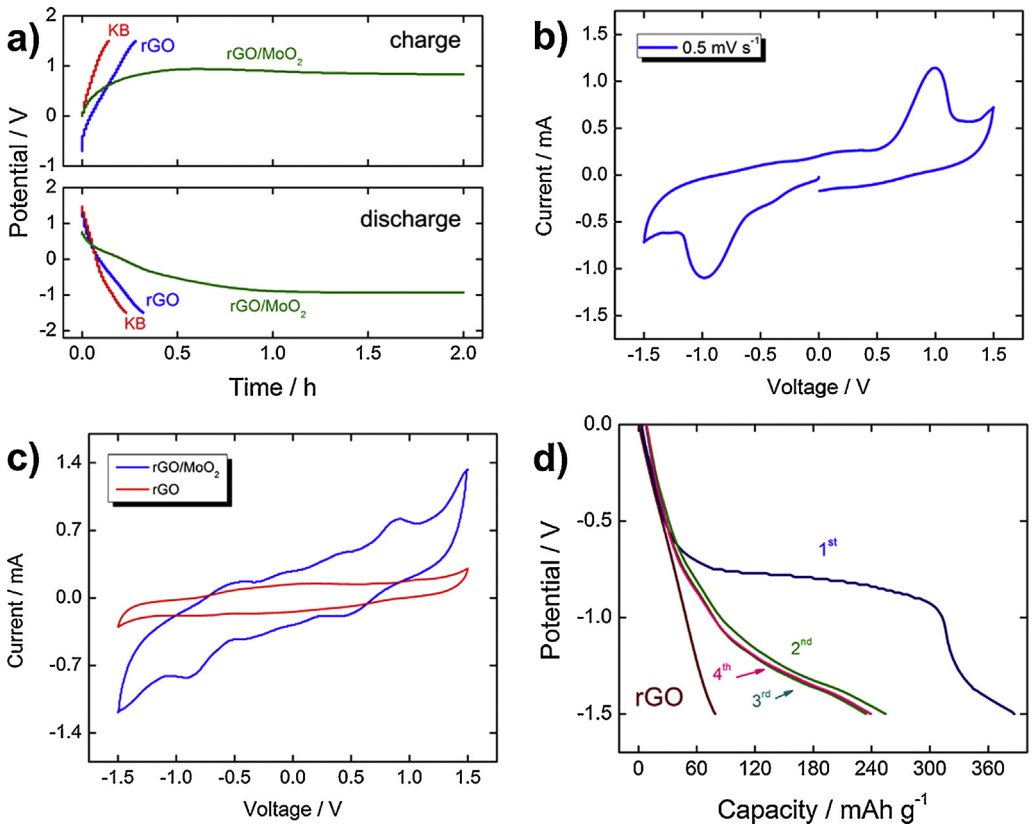

Fig. 3. (a) First charge and discharge profiles of the hybrid, carbon black (KB) and RGO electrodes at a current of 0.5 mA up to 1 mAh. (b) First cycle CV profile of the hybrid electrode and (c) sixth cycle CV profiles of the hybrid (blue) and RGO (red) electrodes. Scan range was from −1.5 V to 1.5 V, and the scan rates was 0.5 mV/s. (d) Galvanostatic discharge profiles of the hybrid electrode for the first 4 cycles (0.5 mA at 1 mAh). First discharge profile of RGO electrode is shown for comparison. (For interpretation of the references to color in this figure legend, the reader is referred to the web version of the article.)

oxidation due to exposure to air, as reported previously [23,24]. The high-resolution O1s spectrum of the hybrid material, reported in Fig. 1 (f), shows the presence of three components, due to the organic component deriving from the residual oxygen bonds to the reduced graphene oxide (C—O at 531.3 eV and C=O at 532.5 eV [24]) and the metal oxide contribution at 530.4 eV. From the latter, it is not possible to resolve the presence of mixed oxide because the peaks for oxygen bonded to Mo (IV) and Mo (VI) are separated by only ~0.2 eV [24–26]. Therefore, a good reduction of GO and molybdenum oxide can be simply achieved by addition of phosphomolybdic acid to the initial dispersion without introducing any further reducing agent like ethylene glycol as reported previously [27]. In addition, as XPS is a surface characterization, it may be postulated that the presence of Mo (VI) is prominent with respect to Mo (IV) only at the surface of nanoparticles because of post-growth surface oxidation, but this fact needs confirmation from a bulk characterization.

In order to unambiguously determine the crystalline phase of molybdenum oxide nanoparticles, TEM and XRD were also employed. For clarity of the analysis, only the molybdenum oxide excess part was collected from the precipitates at the bottom of the hydrothermal reactor. Fig. 2 (a) shows a bright field TEM image of the molybdenum oxide powders. HRTEM in Fig. 2 (b) shows polycrystalline nature of the molybdenum oxide powders with average radius of approximately 150 nm. The XRD data in Fig. 2 (c) suggest the presence of monoclinic molybdenum (IV) oxide in the powders according to JCPDS 32-0671. As XRD is a bulk characterization, the fact that only Mo(IV) contribution was detected confirms that the Mo (VI) revealed by XPS was only present at the surface of nanoparticles. The presence of MoO_2 in the hybrid material was also confirmed by Micro-Raman spectroscopy (Fig. 2 (d)), which showed D, G and 2D bands typical of carbon material [28] at 1345, 1595 and 2694 cm^{-1} respectively. The D band presented a higher intensity than the G band, implying a substantial degree of disorder resulting from the structural defects at the surface and edges of RGO flakes [28,29]. Molybdenum oxide peaks were also present at 284, 337, 376, 663, 820 and 993 cm^{-1}, which suggests a monoclinic structure [22]. This is in good agreement with the XRD data. The composition of the hybrid was determined by TGA, showing a relatively stable thermal behavior up to 400 °C. A sharp weight loss takes place above 450 °C due to the pyrolysis of the carbon component, to be then stabilized to a plateau due to the presence of the molybdenum oxide. From the plateau, the composition of the hybrid was estimated to be approximately 28 wt% Molybdenum oxide.

The electrochemical performance of the hybrid materials was evaluated using a two symmetric electrode configuration, considered a good approximation of the final device. This set-up was preferred to the three-electrode configuration previously adopted in other works [27] in order to avoid large errors in the evaluation of the capacitance values, as suggested by Stoller and Ruoff [30]. Electrodes of pure KB or RGO were used as reference electrodes. Fig. 3 (a) shows GCD profiles of three different electrodes. Both KB and RGO electrodes show rapid polarization with potential changes of 2–3 V within approximately 0.25 h. Strikingly, the hybrid electrode shows a plateau of potential near ±0.9 V during charge (or discharge). This implies that the molybdenum oxide in the hybrid facilitates redox reactions, which likely involved with the insertion of Na ions. Previously lithium ion insertion to the MoO_2 containing electrodes, which is associated with the monoclinic–orthorhombic–monoclinic phase transition of MoO_2, has been reported [29].

The first cycle CV result in Fig. 3 (b) confirms the redox reactions of the hybrid electrode. Clear reduction/oxidation peaks are observed at the potential of approximately −0.9 V and +0.9 V. Fig. 3 (c) shows the sixth cycle CV profiles with scan rate of 0.5 mV/s. The behavior of the hybrid electrode is directly compared with that of RGO electrode. In contrast to the first cycle CV, the sixth cycle CV of the hybrid electrode shows lower redox peaks at ±0.9 V along with multiple redox peaks throughout the potential scan range. It is noted that the RGO electrode shows typical double-layer capacitor behavior without redox peaks. The hybrid electrode gives approximately three times higher specific capacitance values. In fact, a specific capacitance value of 381 F/g has been achieved with hybrid electrodes at a scan rate of 0.5 mV/s compared to 140 F/g, obtained with RGO electrodes, and this trend was observed also at higher scan rates. It is believed that the increase in surface area resulting from molybdenum oxide hybridization, redox reaction of the molybdenum oxide, and possible insertion of Na ion to the molybdenum oxide attribute to this increase in specific capacity. Therefore, we demonstrate that fairly good specific capacitance values can be obtained using a sodium-based aqueous electrolyte, which is less conductive compared to others like KOH and H_2SO_4. In addition, with Na_2SO_4 it is possible to achieve almost double amplitude of stable voltage window, which improves the energy density values of the final device [31]. It is also noted that the hybrid electrode has lower equivalent series resistance (ESR) measured by EIS than that of RGO electrode, respectively 140 and 250 Ohm, implying changes in conductivity resulting from the molybdenum oxide hybridization of the RGO. It is important to notice that these performances were obtained from electrodes made without adding any conductive agent (black carbon, acetylene black, etc.) to the formulation of the paste.

Galvanostatic discharge profiles of the supercapacitor up to 4 cycles are shown in Fig. 3 (d). The first discharge profile of RGO is shown as well as used for comparison. For the hybrid electrode, the first discharge profile is very different from the rest of the profiles. A potential plateau of approximately −0.75 V was observed along with larger capacity than the rest of cycles. A rapid potential drop was observed near capacity value of 300 mAh/g. The plateau in potential is very similar to that observed previously for the ion insertion to the metal oxide. It is believed that the plateau in the first discharge is resulting from the transition from MoO_2 to Na_xMoO_2 by the insertion of Na^+ ions to the molybdenum oxide. Our trial to obtain detailed structural changes resulting from the Na ion insertion using HRTEM, EDS and XRD, however, was not fully successful. That was believed partly to be due to small amount of ion insertion and fair amount of contamination on the electrode (such as salt, for example) during the sample preparation. For the cycles of 2nd to 4th, even though the capacity of the hybrid electrode is higher than that of RGO electrode, no clear potential plateau was observed. This suggests that there were non-reversible electrochemical reactions during the very first galvanic discharge, which might be related to the formation of a solid electrolyte interface layer similar to lithium ion battery electrodes [29,32,33].

4. Conclusions

We prepared a conductive, highly porous graphene-molybdenum oxide hybrid using a facile one-pot hydrothermal synthesis. Structural characterization indicates the formation of polycrystalline nanoparticles of molybdenum oxide on reduced graphene oxide surface. The molybdenum oxide of the hybrid facilitates redox reaction possibly associated with Na^+ ion insertion in aqueous electrolyte. The redox reaction with the hybrid electrode is not fully reversible and results in cycle time dependent discharge behavior. The fact that the hybridization lowers impedance and increases the specific capacity is intriguing for designing an improved supercapacitor using RGO-metal oxide hybrid electrodes.

Acknowledgments

The support of Nagaphani Aetukuri and Andy Tek (IBM Almaden Research Center) in helping respectively with XRD and TGA measurements is gratefully acknowledged.

References

[1] BP, BP Statistical Review of World Energy, 63rd ed., BP Statistical Review of World Energy BP p.l.c., London, 2014.
[2] U.S. Energy Information Administration (EIA), International Energy Outlook 2013 with Projections to 2040. Washington, DC, 2013.
[3] A.K. Shukla, A. Banerjee, M.K. Ravikumar, A. Jalajakshi, Electrochemical capacitor: technical challenges and prognosis for future markets, Electrochim. Acta 84 (2012) 165–173.
[4] Office of Basic Energy Sciences Department of Energy, Basics Research Needs for Electrical Energy Storage. Report of the Basic Energy Sciences Workshop for Electrical Energy Storage, 2007.
[5] P. Simon, Y. Gogotsi, Materials for electrochemical capacitors, Nat. Mater. 7 (2008) 845–854.
[6] A.G. Pandolfo, A.F. Hollenkamp, Carbon properties and their role in supercapacitors, J. Power Sources 157 (2006) 11–27.
[7] G.G. Wallace, J. Chen, D. Li, S.E. Moulton, J.M. Razal, Nanostructured carbon electrodes, J. Mater. Chem. 20 (2010) 3553–3562.
[8] K. Naoi, P. Simon, New materials and new configurations for advanced electrochemical capacitors, Electrochem. Soc. Interface 17 (2008) 34–37.
[9] G. Wang, L. Zhang, J. Zhang, A review of electrode materials for electrochemical supercapacitors, Chem. Soc. Rev. 41 (2012) 797–828.
[10] K. Naoi, W. Naoi, S. Aoyagi, J. Miyamoto, T. Kamino, New generation "nanohybrid supercapacitor", Acc. Chem. Res. 46 (2013) 1075–1083.
[11] L. Zhang, G. Shi, Preparation of highly conductive graphene hydrogels for fabricating supercapacitors with high rate capability, J. Phys. Chem. C 115 (2011) 17206–17212.
[12] Y. Xu, K. Sheng, C. Li, G. Shi, Self-assembled graphene hydrogel via a one-step hydrothermal process, ACS Nano 4 (2010) 4324–4330.
[13] K. Sheng, Y. Xu, C. Li, G. Shi, High-performance self-assembled grapheme hydrogels prepared by chemical reduction of graphene oxide, New Carbon Mater. 26 (2011) 9–15.
[14] Y. Zhao, C. Hu, Y. Hu, H. Cheng, G. Shi, L. Qu, A versatile, ultralight, nitrogen-doped grapheme framework, Angew. Chem. Int. Ed. 51 (2012) 11371–11375.
[15] R. Giardi, S. Porro, A. Chiolerio, E. Celasco, M. Sangermano, Inkjet printed acrylic formulations based on UV-reduced grapheme oxide nanocomposites, J. Mater. Sci. 48 (2013) 1249–1255.
[16] I. Roppolo, A. Chiappone, K. Bejtka, E. Celasco, A. Chiodoni, F. Giorgis, et al., A powerful tool for graphene functionalization: benzophenone mediated UV-grafting, Carbon 77 (2014) 226–235.
[17] Y. Zhou, Q. Bao, L.A.L. Tang, Y. Zhong, K.P. Loh, Hydrothermal dehydration for the "green" reduction of exfoliated graphene oxide to graphene and demonstration of tunable optical limiting properties, Chem. Mater. 21 (2009) 2950–2956.
[18] X. Zhou, L.J. Wan, Y.G. Guo, Synthesis of MoS_2 nanosheet–graphene nanosheet hybrid materials for stable lithium storage, Chem. Commun. 49 (2013) 1838–1840.
[19] Y.J. Lee, D. Barrera, K. Luo, J.W.P. Hsu, In situ chemical oxidation of ultrasmall MoO_x nanoparticles in suspensions, J. Nanotechnol. 61 (2012) 1957.
[20] C.D. Wanger, W.M. Riggs, L.E. Davis, J.F. Moulder, G.E. Muilenberg, Handbook of X-Ray Photoelectron Spectroscopy, Physical Electronics Division, Perkin-Elmer, Waltham, 1979.
[21] R.B. Quincy, M. Houalla, A. Proctor, D.M. Hercules, Distribution of molybdenum oxidation states in reduced Mo/TiO_2 catalysts: correlation with benzene hydrogenation activity, J. Phys. Chem. 94 (1990) 1520–1526.
[22] Y. Liu, H. Zhang, P. Ouyang, L. Zhicheng, One-pot hydrothermal synthesized MoO_2 with high reversible capacity for anode application in lithium ion battery, Electrochim. Acta 102 (2013) 429–435.
[23] B.C. Gates, H. Knozinger, F.C. Jentoft, Advances in Catalysis, Academic Press, Amsterdam, 2009.
[24] Y. Sun, X. Hu, W. Luo, Y. Huang, Ultrafine MoO_2 nanoparticles embedded in a carbon matrix as a high-capacity and long-life anode for lithium–ion batteries, J. Mater. Chem. 22 (2012) 425–431.
[25] J. Swiatowska-Mrowiecka, S. De Diesbach, V. Maurice, S. Zanna, L. Klein, E. Briand, I. Vickridge, P. Marcus, Li-ion intercalation in thermal oxide thin films of MoO_3 as studied by XPS, RBS, and NRA, J. Phys. Chem. C 112 (2008) 11050–11058.
[26] G.E. Buono-Core, A.H. Klahn, C. Castillo, E. Munoz, C. Manzur, G. Cabello, B. Chornik, Synthesis and characterization of thin molybdenum oxide films

prepared from molybdenum dioxotropolonate precursors by photochemical metal–organic deposition (PMOD) and its evaluation as ammonia gas sensors, J. Non-Cryst. Solids 387 (2014) 21–27.
[27] P. Lu, D. Xue, MoO_2/reduced graphene oxide composite electrode with improved cycling performance and high capacitance for supercapacitors, J. Nanoeng. Nanomanuf. 3 (2013) 73–78.
[28] S. Porro, S. Musso, M. Giorcelli, A. Tagliaferro, S.H. Dalal, K.B.K. Teo, et al., Study of CNTs and nanographite grown by thermal CVD using different precursors, J. Non-Cryst. Solids 352 (2006) 1310–1313.
[29] A. Ferrari, Raman spectroscopy of graphene and graphite: disorder, electron–phonon coupling, doping and nonadiabatic effects, Solid State Commun. 143 (2007) 47–57.
[30] M.D. Stoller, R.S. Ruoff, Best practice methods for determining an electrode material's performance for ultracapacitors, Energy Environ. Sci. 3 (2010) 1294–1301.
[31] L. Demarconnay, E. Raymundo-Pinero, F. Béguin, A symmetric carbon/carbon supercapacitor operating at 1.6 V by using a neutral aqueous solution, Electrochem. Commun. 12 (2010) 1275–1278.
[32] Y. Xu, R. Yi, X. Wu, M. Dunwell, Q. Lin, L. Fei, et al., High capacity MoO_2/graphite oxide composite anode for lithium–ion batteries, J. Phys. Chem. Lett. 3 (2012) 309–314.
[33] I.A. Courtney, J.R. Dahn, Electrochemical and in situ X-ray diffraction studies of the reaction of lithium with tin oxide composites, Electrochem. Soc. 144 (1997) 2045–2052.